

**Figure 4. Modulation of regional characteristics of hNCCs.** A) Schematic representation of culture conditions for the induction and maintenance of hNCCs. RA, retinoic acid (100 nM). B) Schematic distribution of marker-positive cells in the murine embryo. DI, diencephalon; MB, midbrain; BA1 to BA4, branchial arch 1 to branchial arch 4; r1 to r6; rhombomere 1 to rhombomere 6. C) The mRNA expression of regional specifier genes in hNCCs.  $p75^{\text{high}}$  cells were collected at the end of the hNCC induction by FACS and seeded onto fibronectin-coated dishes. RNAs were extracted when cells reached a semi-confluent state and used for RT-qPCR. The relative expression level of each gene was demonstrated using the value of cells cultured in CDM (OTX2 and DLX1) or CDM + RA (HOXA2 and HOXA3) as 1.0. Average  $\pm$  SD. N5 3, biological triplicate.

doi:10.1371/journal.pone.0112291.g004

The effects of SB, which has been shown to inhibit Activin/Nodal/TGF $\beta$  signaling and induce neural cells and hNCCs from hPSCs without the help of other chemicals, were firstly evaluated [14]. In accordance with the reported data,

CDM supplemented with SB successfully delivered  $p75^{\text{high}}$  cells with a PAX6-positive neuroectoderm from 201B7 (date not shown), while the induction efficiency of  $p75^{\text{high}}$  cells was approximately 35% (0 nM in [Figure 1C](#)). The activation of Wnt signaling was previously shown to play a key role in the induction of hNCCs [[14](#), [15](#)], and can be achieved using the GSK3b inhibitor BIO or CHIR. Therefore, we attempted to determine the most effective concentration of CHIR with a fixed concentration of SB (10 nM) to induce  $p75^{\text{high}}$  cells. The results obtained revealed that CHIR successfully induced  $p75^{\text{high}}$  cells in a dose-dependent manner up to 1 nM, whereas higher concentrations of CHIR markedly inhibited the production of  $p75^{\text{high}}$  cells ([Figure 1C](#)). We finally examined the effects of BMP signaling on this induction. The addition of BMP4 markedly inhibited the production of  $p75^{\text{high}}$  cells, and these results were compatible with BMP signal inhibiting neural differentiation ([Figure S1A](#)). However, the treatment with DMH1 (10 nM), a specific inhibitor of SMAD1/5/8 phosphorylation, also reduced the  $p75^{\text{high}}$  fraction ([Figure S1B](#)). The inhibitory effect of DMH1 on the induction of  $p75$  was confirmed at different dosages, and other cytoplasmic (LDN193189) or extracellular (Noggin) inhibitors for BMP signaling also decreased the efficiency ([Figure S1C](#)). Therefore, the combination of SB (10 nM) and CHIR (1 nM) most effectively induced  $p75^{\text{high}}$  cells from 201B7 hiPSCs. This result was reproduced in other hPSCs such as hESCs (H9, KhES1, and KhES3) and episomal hiPSCs (414C2) ([Figure 1D](#)). Most cells outgrowing from colonies were stained with NCC markers,  $p75$  and TFAP2A, whereas the cells in colonies were positive for PAX6, a marker for the neuroectoderm ([Figure 1E](#)).

### $p75^{\text{high}}$ cells expressed early NCC markers

The expression of marker genes were compared between  $p75^{\text{high}}$  and  $p75^{\text{low}}$  cells ([Figure 2A](#)). Sorted  $p75^{\text{high}}$  cells expressed a number of genes in the early stage of NCCs, such as SOX10, TWIST1, and TFAP2A genes. In contrast, the expression of these genes was significantly lower in the  $p75^{\text{low}}$  fraction than in  $p75^{\text{high}}$  fraction. The expression of PAX3, which is a marker both for NCCs and neurons, was high in both the  $p75^{\text{high}}$  and  $p75^{\text{low}}$  fractions. The expression of PAX6 and SOX1, which are neural markers, was higher in the  $p75^{\text{low}}$  fraction, which is consistent with some populations of  $p75$ -negative or TFAP2A-negative cells expressing PAX6 ([Figure 1E](#)). These results indicated the relative enrichment of NCC cells in the  $p75^{\text{high}}$  cell population.

In an attempt to further characterize  $p75^{\text{high}}$  cells, genome-wide expression profiles were compared between sorted  $p75^{\text{high}}$  cells and their corresponding hPSCs using a cDNA microarray (Affymetrix Gene 1.0 ST), and we found that the overall profiles of  $p75^{\text{high}}$  cells derived from several PSCs were similar to each other ([Figure S2](#)). Based on the previous report [[32](#)], 46 genes were selected as markers for distinct NC-subpopulations and the expression level of these genes were compared between hNCCs and parental PSCs ([Figure 2B](#)). hNCCs in this study highly expressed early stage-related genes such as neural plate border specifier (PAX3) and NC specification (SNAI2, NGFR, TFAP2A, SOX9, and

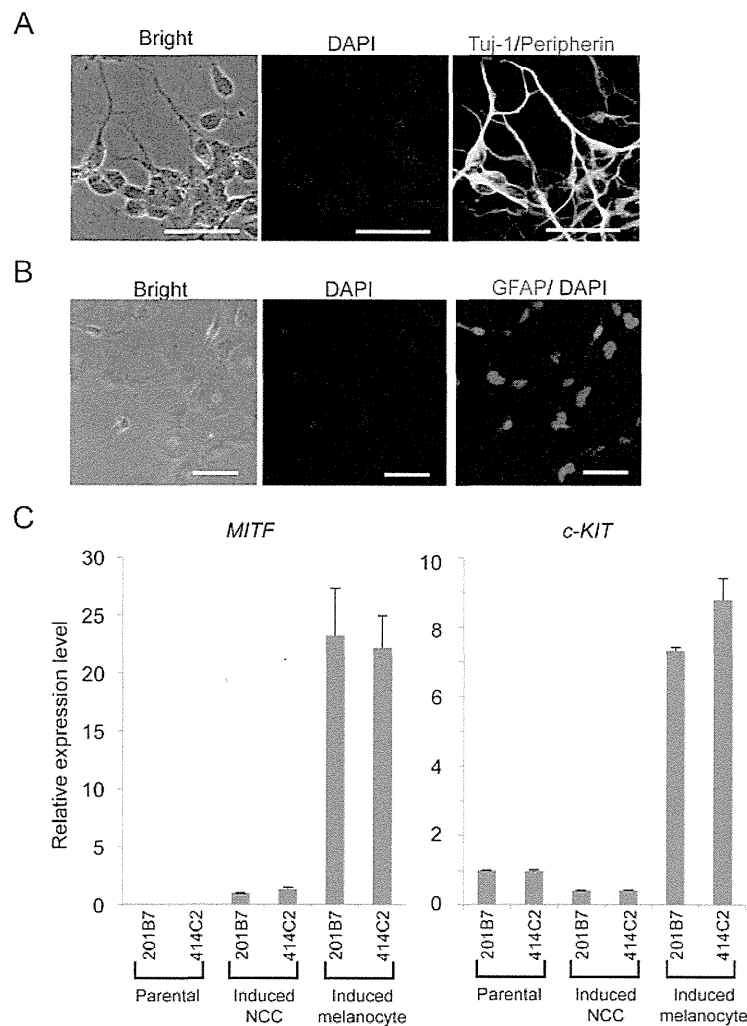


**Figure 5. Derivation of peripheral neural cells, glia, and melanocytes from hNCCs.** A) Neuronal differentiation of 201B7-derived hNCCs. Cells were stained with an antibody against peripherin (red) and Tuj-1 (green). B) The glial differentiation of 201B7-derived hNCCs. Cells were stained with an antibody against GFAP. Scale bar, 50  $\mu$ m. C) Melanocyte differentiation of 201B7-derived hNCCs. The mRNA expression levels of MITF and c-KIT genes were shown as a relative value using the value in 201B7-derived hNCCs and 201B7 as 1.0, respectively. Average  $\pm$  SD. N5 3, biological triplicates.

doi:10.1371/journal.pone.0112291.g005

SOX10), but also some region-specifying genes (EFNB2 for cranial, PDGFRA for cardiac, and SOX5 for trunk region), suggesting the heterogeneous population of p75<sup>high</sup> cells, which were designated hNCCs hereafter. The profiles of the current hNCCs were compared with those of two PSC-derived NCCs, which were induced by different protocols in previous studies [15, 32] (Figure S3). Although the three types of PSC-derived NCCs all highly expressed some genes, such as SNAI2, their

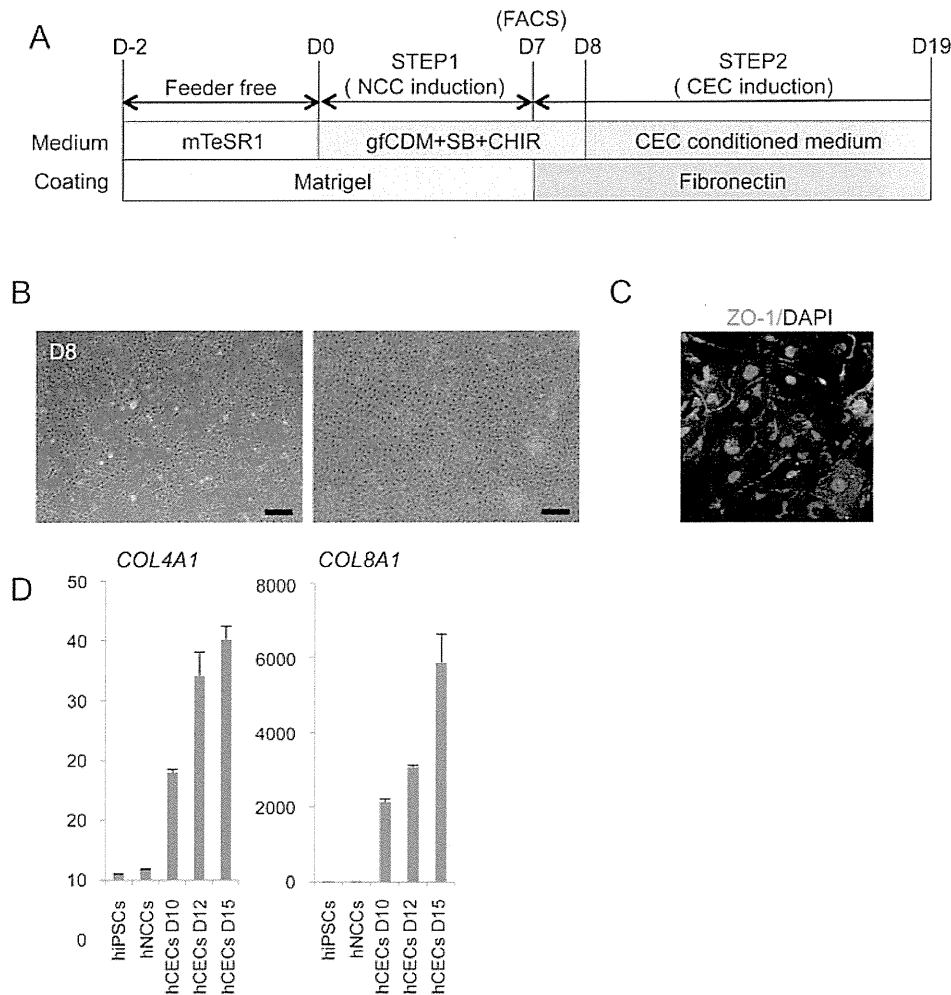


Figure 6. Derivation of corneal endothelial cells from hNCCs. A) Schematic protocol for the induction of corneal endothelial cells. B) Phase contrast images of cells before (D8) and after (D19) the induction. Scale bar; 200  $\mu$ m. C) The expression of ZO-1 in cells at D12. Cells were stained with an antibody against ZO-1. D) The mRNA expression of corneal endothelial cell marker genes. RNAs were extracted from cells at D10, D12, and D15. The expression level of each gene was demonstrated as a relative value using the value in human primary corneal endothelial cells as 1.0. Average  $\pm$  SD. N5 3, technical triplicate. We performed this CEC induction twice and confirmed its reproducibility.

doi:10.1371/journal.pone.0112291.g006

expression profiles were considerably different, suggesting the protocol-dependent heterogeneity of PSC-derived NCCs.

### Sustained expansion of hNCCs with original characteristics

We investigated whether hNCCs could be stably expanded. The growth of hNCCs cultured in the hNCC induction medium (CDM with SB and CHIR) was very slow (data not shown). We employed a cultured condition using CDM supplemented with SB, EGF (20 ng/ml), and FGF2 (20 ng/ml) based on the

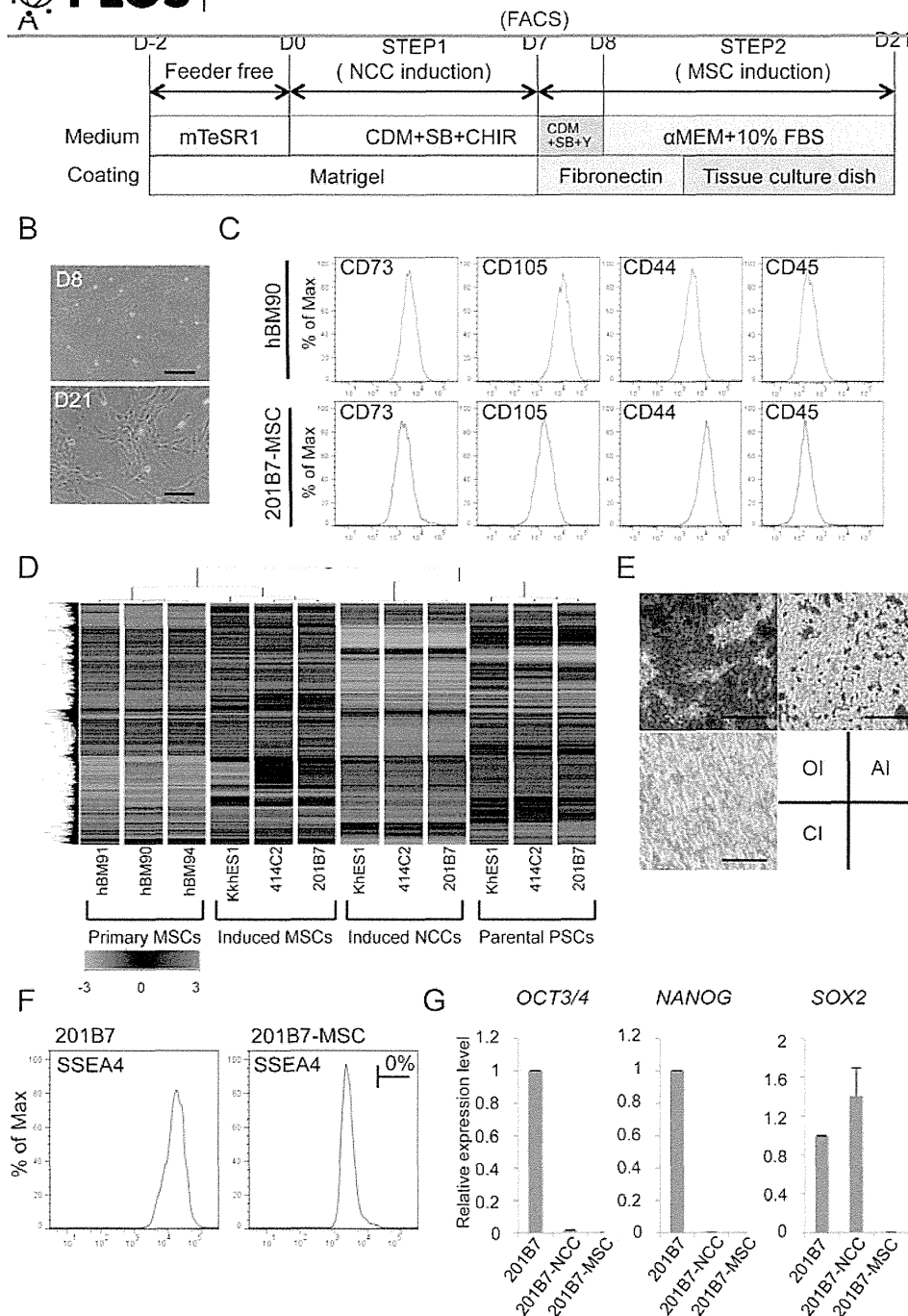


**Figure 7. Derivation of hMSCs from hNCCs.** A) Schematic protocol for the induction of hMSCs. B) Phase contrast images of cells before (D8) and after (D21) the induction. Scale bar, 200 μm. C) Expression of surface markers in hBM-MSCs (hBM90) and 201B7-derived MSCs (201B7-MSC). D) Hierarchical clustering analyses by genome-wide gene expression profiles. RNAs were extracted from hBM-MSCs (BM90, BM91 and BM94), induced-MSCs, and the corresponding hNCCs and hiPSCs. E) Differentiation properties of induced-MSCs. The induction for osteogenic (OI), chondrogenic (CI), and adipogenic (AI) lineages was performed as described in the Materials and Methods section and evaluated by Alizarin Red staining (OI), Alcian Blue staining (CI), and Oil Red O staining (AI), respectively. Scale bar, 100 μm. F) Population of SSEA4-positive cells. G) The expression levels of pluripotent markers (OCT3/4, NANOG and SOX2) in hPSCs, hNCCs, and hMSCs. Average ± SD. N5 3, biological triplicates.

doi:10.1371/journal.pone.0112291.g007

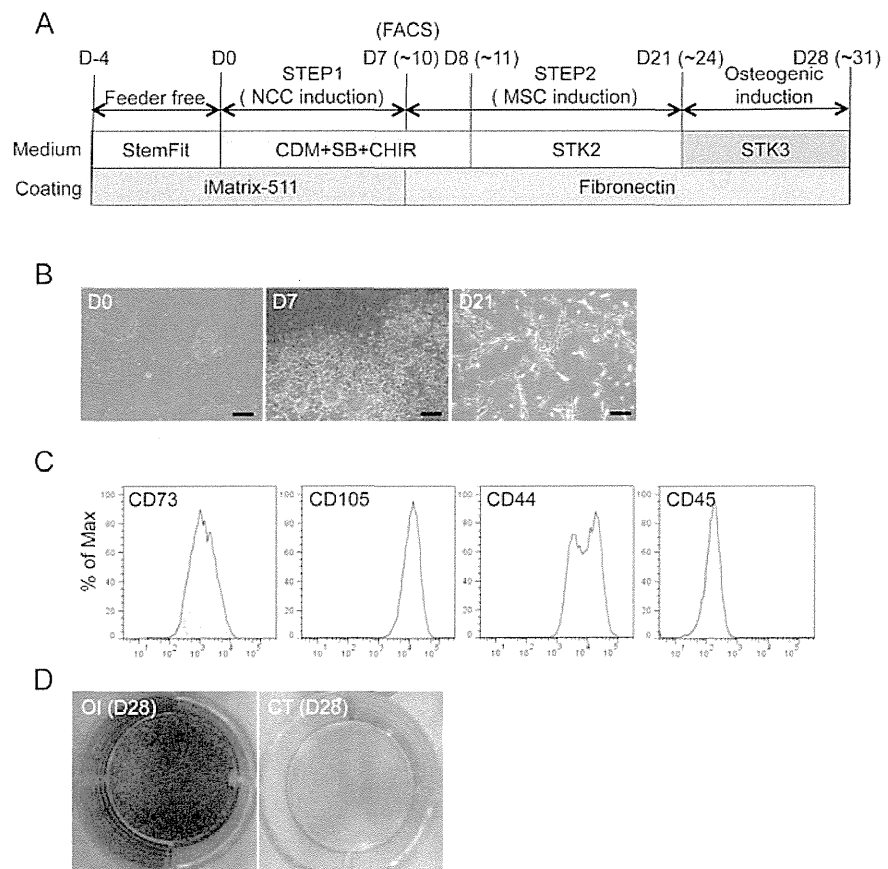


Figure 8. Derivation of hMSCs from hNCCs under defined culture conditions. A) Schematic protocol for the induction of hMSCs from hNCCs under defined culture conditions. B) Phase contrast images of cells 0, 7, and 21 days after the hNCC and hMSC induction, respectively. Scale bar, 200  $\mu$ m. C) Expression of hMSC-related surface markers in hMSCs induced under defined culture conditions. D) Osteogenic differentiation (OI) properties of hMSCs induced under defined culture conditions. hMSCs were cultured during the induction period in STK2 as a control.

doi:10.1371/journal.pone.0112291.g008

findings of previous studies [33], and consequently observed marked improvements in growth and the stable proliferation of hNCCs even after 10 passages (Figures 3A, B). The expanded hNCCs maintained their original cell morphology and all cells expressing NCC markers, such as TFAP2A (Figure 3C). The global gene expression profiles of hNCCs after prolonged expansion (PN10) were similar to those of early passage cells (PN0) (Figure S4A and S4B, correlation coefficient 0.96 to 0.98) and markedly different from those of original hPSCs (Figures 3D and S4C).

## Modulation of the characteristics of hNCCs by insulin and retinoic acid (RA)

The results of the microarray analyses revealed that induced hNCCs expressed some genes characteristic to cranial NCCs (high for OTX2 and DLX1; low for HOXA2 and HOXA3) (date not shown). A previous study demonstrated that the depletion of insulin from CDM (growth-factor free CDM; hereafter referred to as gfCDM) induced a more anterior neuroectoderm (rostral hypothalamic progenitor-like cells), while retinoic acid (RA) exhibited posteriorizing activity [15]. Therefore, we compared the expression of regional markers in hNCCs cultured with gfCDM, CDM, and CDM with RA (100 nM) (Figure 4A). As expected, the expression of OTX2, a marker for mesencephalic NCCs (Figure 4B) [34], was slightly higher under the gfCDM condition than under the CDM condition (Figure 4C). The DLX1 gene, a marker for first and second branchial arch NCCs (Figure 4B) [35], was expressed in cells cultured under all conditions, and was the highest in CDM with the RA condition (Figure 4C). The expression of the HOXA2 and HOXA3 genes, which are markers of the second and third branchial arches, was negligible under the gfCDM and CDM conditions (Figures 4B, C) [36, 37]. Taken together, these results indicated that the regional identities of hNCCs could be modulated by exogenous signals including insulin and RA.

## Derivation of peripheral neurons, glia, and melanocytes from hNCCs

We next examined the differentiation potentials of induced hNCCs. Neuronal differentiation was initiated by sphere formation and promoted by culture media containing a mixture of factors (BDNF, GDNF, NGF, and NT-3). Cells expressed  $\beta$ -tubulin and peripherin after 14 days, which indicated differentiation into peripheral neurons (Figure 5A). Further cultivation under the same conditions (4 to 6 weeks) promoted the glial differentiation of hNCCs (Figure 5B).

Melanocytes are well-known derivatives of NCCs. Using a previously described method that included CHIR, EDN3, and BMP4 [15, 38], induced hNCCs expressed microphthalmia-associated transcription factor (MITF) and *c-KIT*, markers for melanocytes (Figure 5C). These differentiation properties were compatible with those of NCCs *in vivo*.

## Derivation of corneal endothelial cells from hNCCs

Cranial NCCs have been shown to exhibit the ability to differentiate into corneal endothelial cells *in vivo* [39, 40]. Therefore, we examined whether hNCCs grown in gfCDM, which preferentially expressed more anterior NCC markers (Figures 4B, C), could differentiate into cells harboring the characteristics of corneal endothelial cells. When 201B7-derived hNCCs were cultured in the conditioned medium of corneal endothelial cells for twelve days (Figure 6A), cells changed their morphology into that of polygonal corneal endothelial-like cells (

[Figure 6B](#)) and started to express the corneal endothelial marker, ZO-1 ([Figure 6C](#)). Descemet's membrane is known to consist of collagen type 4 and collagen type 8, which are derived from the corneal endothelium [41]. The mRNA expression of the COL4A1 and COL8A1 genes was confirmed in induced endothelial-like cells ([Figure 6D](#)). These results strongly suggested that the hNCCs induced in this study possessed the characteristics of cranial NCCs, which exhibit the potential to differentiate into cranial NCC-derived structures.

### Derivation of hMSCs from hNCCs

Cranial NCCs also have differentiation properties toward mesenchymal cells, which construct the cranio-facial skeleton, and may be referred as MSCs [3]. In order to derivate hMSCs from hNCCs, the culture medium was changed from that for hNCC to aMEM with 10% FBS ([Figure 7A](#)), which we used previously for human bone marrow-derived MSCs (hBM-MSCs) [24]. Through the induction of hMSCs, the expression of NGFR and SOX10 reduced rapidly within 48 hours (PN0) of the medium change, while that of PAX3 and TFAP2A reduced gradually until passage 3 ([Figure S5A](#)). Conversely, the expression of MSC markers (CD73, CD105, and CD44) increased rapidly within 48 hours, reached a maximum by passage number 2, and maintained their expression at a level comparable to that in EMMSCs ([Figure S5B](#)). These results indicated that the transition from NCCs to MSCs was gradual during passage number three. Cells passaged three times in the medium showed a typical fibroblastic morphology similar to that of hMSCs ([Figure 7B](#)), and expressed surface markers for hMSCs (positive for CD73, CD105, and CD44, and negative for CD45) ([Figure 7C](#)). Microarray analyses revealed that hNCC-derived MSCs had a global expression pattern similar to that of primary hBM-MSCs ([Figure 7D](#)). Differentiation properties toward osteogenic, chondrogenic, and adipogenic lineages are one of the criteria required for MSCs [42], which were clearly confirmed in hNCC-derived MSCs ([Figure 7E](#)). FACS analysis showed that there was no SSEA4-positive cells ([Figure 7F](#)) and the expression of PSC marker genes was below detectable levels ([Figure 7G](#)).

### Derivation of osteogenic cells from hiPSCs under defined culture conditions

We determined the feasibility of inducing terminally differentiated cells from iPSCs under defined culture conditions ([Figure 8](#)). 987A3 hiPSCs were used as the initial material, which have been generated and maintained under feeder-free and xeno-free conditions [21]. Cells were dissociated into single cells, seeded on iMatrix-coated dishes (0.83–1.35 cells/cm<sup>2</sup>), and cultured with StemFit medium for five days. hNCCs were then induced for seven to ten days ([Figure 8A](#)). The efficiency of hNCC induction under these conditions was  $40.9 \pm 5.5\%$  ( $\pm$  SD, N5 3, biological triplicate). The induction of hMSCs was performed using CDM for MSCs (STK2) instead of aMEM/10% FBS ([Figure 8A](#)). After several passages of hNCCs in STK2, the morphology of cells changed from cuboidal to fibroblastic,



similar to that of hBM-MSCs (Figure 8B). The expression patterns of surface markers were compatible with those of hMSCs (positive for CD73, CD105, and CD44, and negative for CD45) (Figure 8C) and the differentiation properties for osteogenic, chondrogenic, and adipogenic lineages were confirmed when the standard FBS-containing induction medium was used (Figure S6). Osteogenic differentiation was also confirmed using the chemically-defined osteogenic medium (STK3) (Figure 8D). These results indicated that all steps from iPSC to osteogenic cells could be performed under defined culture conditions.

## Discussion

In the present study, we developed a simple and efficient induction method for hNCCs from hPSCs. The induction efficiency of this method was high (70–80%) irrespective with the type of hPSC. The induced hNCCs exhibited the cranial NCC characters under maintenance culture conditions, while further treatment with insulin and RA marginally posteriorized hNCCs. Consistent with the expression of cranial NCC markers, induced hNCCs could differentiate into corneal endothelial cells, which is a characteristic of cranial NCCs.

Our protocol was independent of the BMP signal. In our protocol, DMH1, a specific BMP inhibitor, clearly attenuated the induction efficiency of the p75<sup>high</sup> fraction (Figure S1). This result clearly contradicted the findings of previous studies (no effect [14] or increased efficiency [15]). The marked differences in the findings of these studies may be attributed to the seeding density used at the beginning of induction. The seeding density of our protocol was approximately 2–4 clumps/cm<sup>2</sup> (approximately 20 cells/cm<sup>2</sup>), while other studies used 16 × 10<sup>4</sup> cells/cm<sup>2</sup> [26]. Both CNS and neural crest fates were previously observed when cells were seeded at a low density, while CNS cells primarily formed at a high density [43]. In accordance with these findings, the efficiency of the NCC induction was markedly decreased if clumps were seeded at a higher density (data not shown). The high density of hNCCs may have exaggerated local BMP signaling secreted from the hNCCs themselves. Therefore, we combined high density seeding with the BMP inhibitor treatment; however, the efficiency was still low (data not shown). Based on these results, we could not account for the differences between our protocol and those of previous studies.

In order to compare the hNCCs in this study with those in previous studies, we analyzed gene expression profiles of hNCCs published previously. The comparison of the relative induction levels of NCC specific genes revealed that hNCCs differentiated by our protocol and previous studies showed similarities in some aspects, but overall profiles were different from each other (Figure S3). These results indicated that induction protocols reported in this study and in the previous studies induced different subset of hNCCs.

Induced hNCCs exhibited differentiation properties for multiple cell lineages including peripheral neurons, glial cells, melanocytes, and corneal endothelial cells, and also delivered hMSCs that further differentiated into osteogenic,

chondrogenic, and adipogenic cells. These properties are compatible with NCCs being multipotent stem cells [3]. However, clonal analyses are indispensable for confirming the stemness of induced hNCCs. Previous clonal analyses revealed that 63–65% of the hNCC clones could differentiate into multi-lineage cells positive for markers of neurons, glial cells, and smooth muscle cells [43, 44], suggesting that hNCCs induced from hPSCs were multipotent on the clonal level. Although stemness has yet to be investigated in this study, induced hNCCs in this protocol will be a promising cell source for various types of research.

Human diseases that have been related to the development of hNCCs include Hirschsprung's disease, DiGeorge syndrome, Waardenburg syndrome, Charcot-Marie-tooth disease, Hermansky-Pudlak syndrome, familial dysautonomia, Chediak-Higashi syndrome, and CHARGE syndrome [45, 46]. hNCCs containing the mutations responsible for these diseases can be induced from hiPSCs established from the respective patients; therefore, this will be a powerful tool for creating in vitro disease models that can contribute to a more detailed understanding of the pathogenesis of NCC disorders and also to the development of novel therapeutic modalities [15]. In addition, hNCCs have been shown to be the cell-of-origin of some cancers such as neuroblastoma [47], which indicates that hNCCs can be used in in vitro transformation experiments. We have already confirmed that the survival rate of freeze-stocked hNCCs was satisfactory and the freeze and thaw process had no impact on the growth and differentiation properties of these cells (data not shown). These are favorable features for a material in research because it is important to use cells of the same quality in order to evaluate reproducibility.

Induced hNCC derivatives can also be used for cell therapy. In this regard, hNCC-derived hMSCs will be a very useful material. hMSCs have been used in a wide range of regenerative medicines, and promising results have been reported in some cases [48, 49]. In contrast with the advances reported in clinical applications, many issues related to the biology of hMSCs have yet to be investigated, one of which is the cell-of-origin of hMSCs. hNCCs may be the precursors of hMSCs based on the finding that craniofacial skeletal tissues are derived from NCCs [50]. This has also been supported in lineage tracing experiments using *P0-cre* mice [51, 52]. Current sources of hMSCs include bone marrow, fat tissue, synovium, and umbilical cord; however, it remains unclear whether NCC-derived cells exist in all of these adult tissues and serve as the source of hMSCs. A comparison between hNCC-derived MSCs and somatic tissue-derived hMSCs may provide more information related to this issue.

One of the limitations of current hMSCs is their limited proliferative activity, which may pose problems in their application to conditions requiring a large amount of cells. This can be overcome if hNCC-derived MSCs are used because hNCCs can be induced from hPSCs, which have unlimited proliferative activity. Two issues are important for this application. One is to be free from infectious substances that may be derived from animal materials. Using iPSCs generated and maintained under feeder-free and xeno-free conditions, we successfully induced hNCCs and hMSCs with minimum animal material (BSA in CDM) (Figure 8A).

Furthermore, we generated terminally differentiated cells (osteogenic cells) from these MSCs under chemically defined media. To the best of our knowledge, this is the first study to demonstrate the induction of osteogenic cells under feeder-free and serum-free conditions from PSCs. The other concern relates to the contamination of undifferentiated cells, particularly parental hPSCs, which may lead to serious conditions such as the formation of malignant tumors [53]. We confirmed that hNCC-derived hMSCs were free from SSEA4-expressing cells and the expression of PSC-marker genes was below detectable levels (Figures 7F, G). Although more precise and meticulous analyses are required to prove the safety of these cells, the results of the present study have provided evidence to promote the use of hNCC-derived hMSCs for cell therapy.

### Supporting Information

**Figure S1.** Effect of the BMP signal on the induction of p75<sup>high</sup> cells. hiPSCs (201B7) were treated in NCC induction media with BMP4 (10 ng/ml) (A) or DMH1 (10 nM) (B), and the fraction of p75-positive cells was analyzed by FACS. C) Effects of BMP signal inhibitors on the induction of p75<sup>high</sup> cells. 201B7 cells were treated with each BMP inhibitor at the indicated dosage, and the fraction of p75-positive cells was analyzed by FACS.

[doi:10.1371/journal.pone.0112291.s001](https://doi.org/10.1371/journal.pone.0112291.s001) (TIFF)

**Figure S2.** Global comparison of the expressions of genes between PSCs and p75<sup>high</sup> cells. A) A volcano plot showing the P value for differences in the expression of each gene between the average of PSC lines (H9, KhES1, 414C2, and 201B7) and the average of corresponding p75<sup>high</sup> cells. A total of 562 entities downregulated and 447 entities upregulated in p75<sup>high</sup> cells were identified as a differentially expressed gene set. B) Heat map analyses revealed global similarities among hNCCs derived from each PSC line.

[doi:10.1371/journal.pone.0112291.s002](https://doi.org/10.1371/journal.pone.0112291.s002) (TIFF)

**Figure S3.** Expression of NCC marker genes in induced NCCs from PSCs. The induction ratio of NCC markers relative to a corresponding pluripotent baseline was demonstrated in each induced NCC. iPS NCCs, GSE44727.

WA09\_NC\_Day11, 45223. Marker genes for each sub-population of NCC were labeled using the indicated colors.

[doi:10.1371/journal.pone.0112291.s003](https://doi.org/10.1371/journal.pone.0112291.s003) (TIFF)

**Figure S4.** Comparison of gene expression profiles between hNCCs at different passages by scatter plotting. RNAs were extracted from hNCCs derived from 201B7 (A) and KhES1 (B) at different passages (PN0, PN4 and PN10), and analyzed using microarrays. C) Correlation coefficient analysis was performed using these data.

[doi:10.1371/journal.pone.0112291.s004](https://doi.org/10.1371/journal.pone.0112291.s004) (TIFF)

**Figure S5.** The expression of markers for hNCCs and hMSCs in each passage. A gradual transition from hNCCs to hMSCs was observed in hNCC markers (A)

and hMSC markers (B). Average  $\pm$  SD. N5 3, biological triplicates. Regarding BMSCs, cDNA was prepared from the bone marrow stromal cells of four healthy donors (BM25, 26, 34, and 107), and the average was presented as BMSCs in each graph.

[doi:10.1371/journal.pone.0112291.s005](https://doi.org/10.1371/journal.pone.0112291.s005) (TIFF)

Figure S6. Osteogenic-, chondrogenic-, adipogenic induction from feeder-free hiPSCs through hNCC-derived hMSCs. Differentiation properties of hNCC-MSCs. The induction for osteogenic (OI), chondrogenic (CI), and adipogenic (AI) lineages was performed as described in the Materials and Methods section and evaluated by Alizarin Red staining (OI), Alcian Blue staining (CI), and Oil Red O staining (AI), respectively. Scale bar, 200  $\mu$ m.

[doi:10.1371/journal.pone.0112291.s006](https://doi.org/10.1371/journal.pone.0112291.s006) (TIFF)

Table S1. Information of primary antibodies used in this study.

[doi:10.1371/journal.pone.0112291.s007](https://doi.org/10.1371/journal.pone.0112291.s007) (TIF)

Table S2. Information of PCR primers used in this study.

[doi:10.1371/journal.pone.0112291.s008](https://doi.org/10.1371/journal.pone.0112291.s008) (TIF)

## Acknowledgments

We thank Dr. H. Tanaka for the kind advice and help in the corneal endothelium induction, M. Shibata, K.R. Komatsu, and J Nakai for their technical assistance, and T. Kato, Y. Jn. S. Tamaki, and S. Hineno for their support during this study.

## Author Contributions

Conceived and designed the experiments: MF NK TN MS TO SK MU MI JT. Performed the experiments: MF YN KK KS SN YM TY NO TS MI. Analyzed the data: MF YN KK NK MU TS MI. Contributed reagents/materials/analysis tools: MN TY KU TH. Wrote the paper: MF YN TY MU MI JT.

## References

1. Liu Z, Tang Y, Lu S, Zhou J, Du Z, et al. (2013) The tumorigenicity of iPS cells and their differentiated derivatives. *J Cell Mol Med* 17: 782–791.
2. Le Douarin NM, Dupin E (2003) Multipotentiality of the neural crest. *Curr Opin Genet Dev* 13: 529–536.
3. Sauka-Spengler T, Bronner-Fraser M (2008) A gene regulatory network orchestrates neural crest formation. *Nat Rev Mol Cell Biol* 9: 557–568.
4. Kalcheim C, Burstyn-Cohen T (2005) Early stages of neural crest ontogeny: formation and regulation of cell delamination. *Int J Dev Biol* 49: 105–116.
5. Kalcheim C (2000) Mechanisms of early neural crest development: from cell specification to migration. *Int Rev Cytol* 200: 143–196.
6. Vincent SD, Buckingham ME (2010) How to make a heart: the origin and regulation of cardiac progenitor cells. *Curr Top Dev Biol* 90: 1–41.

7. Neirinckx V, Coste C, Rogister B, Wislet-Gendebien S (2013) Concise review: adult mesenchymal stem cells, adult neural crest stem cells, and therapy of neurological pathologies: a state of play. *Stem Cells Transl Med* 2: 284–296.
8. Neirinckx V, Marquet A, Coste C, Rogister B, Wislet-Gendebien S (2013) Adult bone marrow neural crest stem cells and mesenchymal stem cells are not able to replace lost neurons in acute MPTP-lesioned mice. *PLoS One* 8: e64723.
9. Giuliani M, Oudrhiri N, Noman ZM, Vernochet A, Chouaib S, et al. (2011) Human mesenchymal stem cells derived from induced pluripotent stem cells down-regulate NK-cell cytolytic machinery. *Blood* 118: 3254–3262.
10. Villa-Diaz LG, Brown SE, Liu Y, Ross AM, Lahann J, et al. (2012) Derivation of mesenchymal stem cells from human induced pluripotent stem cells cultured on synthetic substrates. *Stem Cells* 30: 1174–1181.
11. Liu Q, Spusta SC, Mi R, Lassiter RN, Stark MR, et al. (2012) Human neural crest stem cells derived from human ESCs and induced pluripotent stem cells: induction, maintenance, and differentiation into functional schwann cells. *Stem Cells Transl Med* 1: 266–278.
12. Chinge NO, Bayarsaihan D (2010) Generation of neural crest progenitors from human embryonic stem cells. *J Exp Zool B Mol Dev Evol* 314: 95–103.
13. Milet C, Monsoro-Burq AH (2012) Embryonic stem cell strategies to explore neural crest development in human embryos. *Dev Biol* 366: 96–99.
14. Menendez L, Yatskievych TA, Antin PB, Dalton S (2011) Wnt signaling and a Smad pathway blockade direct the differentiation of human pluripotent stem cells to multipotent neural crest cells. *Proc Natl Acad Sci U S A* 108: 19240–19245.
15. Mica Y, Lee G, Chambers SM, Tomishima MJ, Studer L (2013) Modeling neural crest induction, melanocyte specification, and disease-related pigmentation defects in hESCs and patient-specific iPSCs. *Cell Rep* 3: 1140–1152.
16. Suemori H, Yasuchika K, Hasegawa K, Fujioka T, Tsuneyoshi N, et al. (2006) Efficient establishment of human embryonic stem cell lines and long-term maintenance with stable karyotype by enzymatic bulk passage. *Biochem Biophys Res Commun* 345: 926–932.
17. Amit M, Carpenter MK, Inokuma MS, Chiu CP, Harris CP, et al. (2000) Clonally derived human embryonic stem cell lines maintain pluripotency and proliferative potential for prolonged periods of culture. *Dev Biol* 227: 271–278.
18. Okita K, Matsumura Y, Sato Y, Okada A, Morizane A, et al. (2011) A more efficient method to generate integration-free human iPSC cells. *Nat Methods* 8: 409–412.
19. Takahashi K, Tanabe K, Ohnuki M, Narita M, Ichisaka T, et al. (2007) Induction of pluripotent stem cells from adult human fibroblasts by defined factors. *Cell* 131: 861–872.
20. McMahon AP, Bradley A (1990) The Wnt-1 (int-1) proto-oncogene is required for development of a large region of the mouse brain. *Cell* 62: 1073–1085.
21. Nakagawa M, Taniguchi Y, Senda S, Takizawa N, Ichisaka T, et al. (2014) A novel efficient feeder-free culture system for the derivation of human induced pluripotent stem cells. *Sci Rep* 4: 3594.
22. Nasu A, Ikeya M, Yamamoto T, Watanabe A, Jin Y, et al. (2013) Genetically matched human iPSC cells reveal that propensity for cartilage and bone differentiation differs with clones, not cell type of origin. *PLoS One* 8: e53771.
23. Wataya T, Ando S, Muguruma K, Ikeda H, Watanabe K, et al. (2008) Minimization of exogenous signals in ES cell culture induces rostral hypothalamic differentiation. *Proc Natl Acad Sci U S A* 105: 11796–11801.
24. Colleoni S, Galli C, Giannelli SG, Armentero MT, Blandini F, et al. (2010) Long-term culture and differentiation of CNS precursors derived from anterior human neural rosettes following exposure to ventralizing factors. *Exp Cell Res* 316: 1148–1158.
25. James MJ, Jarvinen E, Wang XP, Thesleff I (2006) Different roles of Runx2 during early neural crest derived bone and tooth development. *J Bone Miner Res* 21: 1034–1044.
26. Lee G, Chambers SM, Tomishima MJ, Studer L (2010) Derivation of neural crest cells from human pluripotent stem cells. *Nat Protoc* 5: 688–701.

27. Ohta S, Imaizumi Y, Okada Y, Akamatsu W, Kuwahara R, et al. (2011) Generation of human melanocytes from induced pluripotent stem cells. *PLoS One* 6: e16182.
28. Fang D, Leishear K, Nguyen TK, Finko R, Cai K, et al. (2006) Defining the conditions for the generation of melanocytes from human embryonic stem cells. *Stem Cells* 24: 1668–1677.
29. Ju C, Zhang K, Wu X (2012) Derivation of corneal endothelial cell-like cells from rat neural crest cells *in vitro*. *PLoS One* 7: e42378.
30. Umeda K, Zhao J, Simmons P, Stanley E, Elefanty A, et al. (2012) Human chondrogenic paraxial mesoderm, directed specification and prospective isolation from pluripotent stem cells. *Sci Rep* 2: 455.
31. Okamoto T, Aoyama T, Nakayama T, Nakamata T, Hosaka T, et al. (2002) Clonal heterogeneity in differentiation potential of immortalized human mesenchymal stem cells. *Biochem Biophys Res Commun* 295: 354–361.
32. Kreitzer FR, Salomonis N, Sheehan A, Huang M, Park JS, et al. (2013) A robust method to derive functional neural crest cells from human pluripotent stem cells. *Am J Stem Cells* 2: 119–131.
33. Lee G, Ramirez CN, Kim H, Zeltner N, Liu B, et al. (2012) Large-scale screening using familial dysautonomia induced pluripotent stem cells identifies compounds that rescue IKBKAP expression. *Nat Biotechnol* 30: 1244–1248.
34. Kimura C, Takeda N, Suzuki M, Oshimura M, Aizawa S, et al. (1997) Cis-acting elements conserved between mouse and pufferfish *Otx2* genes govern the expression in mesencephalic neural crest cells. *Development* 124: 3929–3941.
35. Qiu M, Bulfone A, Ghattas I, Meneses JJ, Christensen L, et al. (1997) Role of the *Dlx* homeobox genes in proximodistal patterning of the branchial arches: mutations of *Dlx-1*, *Dlx-2*, and *Dlx-1* and *-2* alter morphogenesis of proximal skeletal and soft tissue structures derived from the first and second arches. *Dev Biol* 185: 165–184.
36. Manley NR, Capecchi MR (1995) The role of *Hoxa-3* in mouse thymus and thyroid development. *Development* 121: 1989–2003.
37. Liu Z, Yu S, Manley NR (2007) *Gcm2* is required for the differentiation and survival of parathyroid precursor cells in the parathyroid/thymus primordia. *Dev Biol* 305: 333–346.
38. Motohashi T, Aoki H, Yoshimura N, Kunisada T (2006) Induction of melanocytes from embryonic stem cells and their therapeutic potential. *Pigment Cell Res* 19: 284–289.
39. Johnston MC, Noden DM, Hazelton RD, Coulobre JL, Coulobre AJ (1979) Origins of avian ocular and periocular tissues. *Exp Eye Res* 29: 27–43.
40. Trainor PA, Tam PP (1995) Cranial paraxial mesoderm and neural crest cells of the mouse embryo: co-distribution in the craniofacial mesenchyme but distinct segregation in branchial arches. *Development* 121: 2569–2582.
41. Fitch JM, Birk DE, Linsenmayer C, Linsenmayer TF (1990) The spatial organization of Descemet's membrane-associated type IV collagen in the avian cornea. *J Cell Biol* 110: 1457–1468.
42. De Schauwer C, Meyer E, Van de Walle GR, Van Soom A (2011) Markers of stemness in equine mesenchymal stem cells: a plea for uniformity. *Theriogenology* 75: 1431–1443.
43. Lee G, Kim H, Elkabetz Y, Al Shamy G, Panagiotakos G, et al. (2007) Isolation and directed differentiation of neural crest stem cells derived from human embryonic stem cells. *Nat Biotechnol* 25: 1468–1475.
44. Curchoe CL, Maurer J, McKeown SJ, Cattarossi G, Cimadamore F, et al. (2010) Early acquisition of neural crest competence during hESCs neuralization. *PLoS One* 5: e13890.
45. Bajpai R, Chen DA, Rada-Iglesias A, Zhang J, Xiong Y, et al. (2010) CHD7 cooperates with PBAF to control multipotent neural crest formation. *Nature* 463: 958–962.
46. Lee G, Papapetrou EP, Kim H, Chambers SM, Tomishima MJ, et al. (2009) Modelling pathogenesis and treatment of familial dysautonomia using patient-specific iPSCs. *Nature* 461: 402–406.
47. Jiang M, Stanke J, Lahti JM (2011) The connections between neural crest development and neuroblastoma. *Curr Top Dev Biol* 94: 77–127.
48. Caplan AI (2007) Adult mesenchymal stem cells for tissue engineering versus regenerative medicine. *J Cell Physiol* 213: 341–347.

49. Silva NA, Sousa N, Reis RL, Salgado AJ (2013) From basics to clinical: A comprehensive review on spinal cord injury. *Prog Neurobiol*.
50. Helms JA, Schneider RA (2003) Cranial skeletal biology. *Nature* 423: 326–331.
51. Morikawa S, Mabuchi Y, Niibe K, Suzuki S, Nagoshi N, et al. (2009) Development of mesenchymal stem cells partially originate from the neural crest. *Biochem Biophys Res Commun* 379: 1114–1119.
52. Takashima Y, Era T, Nakao K, Kondo S, Kasuga M, et al. (2007) Neuroepithelial cells supply an initial transient wave of MSC differentiation. *Cell* 129: 1377–1388.
53. Cai J, Yang M, Poremsky E, Kidd S, Schneider JS, et al. (2010) Dopaminergic neurons derived from human induced pluripotent stem cells survive and integrate into 6-OHDA-lesioned rats. *Stem Cells Dev* 19: 1017–1023.

# Survival and Neurodevelopmental Outcome of Preterm Infants Born at 22–24 Weeks of Gestational Age

Masayuki Ochiai<sup>a,c</sup> Tadamune Kinjo<sup>a,c</sup> Yasushi Takahata<sup>a</sup> Mariko Iwayama<sup>a</sup>  
Takeru Abe<sup>b</sup> Kenji Ihara<sup>a,c</sup> Shouichi Ohga<sup>c,f</sup> Kotaro Fukushima<sup>a,d</sup>  
Kiyoko Kato<sup>a,d</sup> Tomoaki Taguchi<sup>a,e</sup> Toshiro Hara<sup>a,c</sup>

<sup>a</sup>Comprehensive Maternity and Perinatal Care Center and <sup>b</sup>Medical Information Center, Kyushu University Hospital, Departments of <sup>c</sup>Pediatrics, <sup>d</sup>Obstetrics and Gynecology, <sup>e</sup>Pediatric Surgery and <sup>f</sup>Perinatal and Pediatric Medicine, Graduate School of Medical Sciences, Kyushu University, Fukuoka, Japan

© S. Karger AG, Basel

**PROOF Copy  
for personal  
use only**

ANY DISTRIBUTION OF THIS  
ARTICLE WITHOUT WRITTEN  
CONSENT FROM S. KARGER  
AG, BASEL IS A VIOLATION  
OF THE COPYRIGHT.

## Key Words

Extremely premature infants · Extremely low birthweight · Mortality · Morbidity · Antenatal steroid

## Abstract

**Background:** The limits of viability in extremely premature infants are challenging for any neonatologists in developed countries. The neurological development and growth of extremely preterm infants have come to be the emerging issue following the management in the neonatal intensive care unit. **Objective:** To assess potential associations between changes in practice and survival/neurodevelopmental outcome, and clinical outcomes of extremely preterm infants born at the limit of viability studied in a tertiary center. **Study Design:** A retrospective study enrolled 51 infants who had no congenital disorders, and were born at 22–24 weeks of gestational age (GA) in 2000–2009 in our institution. Clinical variables and interventions were studied with regard to one-year survival and developmental quotient (DQ) at 3 years of age. **Results:** The one-year survival rate of 24 preterm infants born in 2005–2009 (79%) was higher than that of the 27 infants born in 2000–2004 (52%,  $p = 0.04$ ). Infants born after 2005 underwent less tocolysis (54 vs. 94%,  $p < 0.01$ ) and

more frequently antenatal steroid therapy (32 vs. 6%,  $p = 0.01$ ) than those born before 2004. The post-2005 survivors ( $n = 19$ ) received more frequently indomethacin therapy (89 vs. 50%,  $p = 0.03$ ) and early parenteral nutrition (95 vs. 36%,  $p < 0.01$ ) than the pre-2004 survivors ( $n = 14$ ). There were no differences in the proportion of infants who attained a DQ of  $>50$  at 3 years of age between pre-2004 (9/13, 69%) and post-2005 groups (10/17, 59%). Multivariate analysis indicated that extremely premature birth at GA  $<24$  weeks was the sole critical factor for a DQ of  $>50$  in survivors. **Conclusions:** The perinatal care after 2005 improved the overall survival rate, but not the neurological outcome of preterm survivors at the limit of viability. Neurodevelopmental impairments were associated with extremely premature birth at GA  $<24$  weeks.

© 2013 S. Karger AG, Basel

## Introduction

Recent progress in the perinatal and neonatal care has greatly improved the prognosis of critically ill or premature newborn infants. The limits of viability in extremely premature infants are challenging for any neonatologist

KARGER

© 2013 S. Karger AG, Basel  
1661-7800/13/0000-0000\$38.00/0

E-Mail [karger@karger.com](mailto:karger@karger.com)  
[www.karger.com/neo](http://www.karger.com/neo)

Masayuki Ochiai, MD, PhD  
Department of Pediatrics, Graduate School of Medical Sciences  
Kyushu University 3-1-1 Maidashi, Higashi-ku  
Fukuoka 812-8582 (Japan)  
E-Mail [ochimasa@pediatr.med.kyushu-u.ac.jp](mailto:ochimasa@pediatr.med.kyushu-u.ac.jp)



in developed countries [1–4]. Between 2004 and 2007, the one-year survival rate of infants born at 22–26 weeks of gestational age (GA) in Sweden attained 70%, ranging from 9.8% at GA 22 to 85% at GA 26 weeks [5]. In 2005, the survival rates of Japanese infants during their stay in a neonatal intensive care unit (NICU) were 34.0, 54.2 and 76.6% in infants born at GA 22, 23, and 24 weeks, respectively [6]. On the other hand, the post-NICU neurological development and growth of extremely preterm infants have come to be the emerging issue.

Antenatal steroid therapy was reportedly associated with a significant decrease in the mortality of preterm infants born at GA 22–23 weeks [7]. This intervention was actively introduced in our tertiary center after 2005 for women at high risk of preterm delivery after GA 22 weeks. The alive-born premature infants are at high-risk for a constellation of life-threatening events including cerebral bleeding and sepsis. A small number of survivors at the limit of viability still have an increased risk of physiological and neurodevelopmental problems requiring long-term medical support and socioeconomical services. To assess potential associations between changes in practice and survival/neurodevelopmental outcome, we performed the present study in all infants born at GA 22–24 weeks and treated at a single tertiary center from 2000 to 2009. The favorable limits of viability and neurodevelopmental outcome are discussed with special reference to the prenatal and postnatal management.

## Materials and Methods

### Study Subjects

The study population included all infants delivered at GA 22–24 weeks at the Kyushu University Hospital in Japan from January 1st 2000 to December 31st 2009 (fig. 1). The maternal and neonatal records of all infants were studied retrospectively. The information collected included previous obstetric history, the present pregnancy and delivery, infant morbidity, treatment, survival, and neurodevelopmental outcome up to 3 years of age. A total of 51 alive infants, all free from congenital diseases, reached the NICU for intensive treatment.

Perinatal period was defined as comprising late pregnancy from GA 22 weeks until birth, labor and delivery, and the first week of life in accordance with the recommendations of the World Health Organization (WHO). Live birth and perinatal mortality were also defined by the WHO recommendations (<http://www.who.int/whr/2005/en/index.html>). Perinatal mortality included stillbirths and early neonatal deaths. Stillbirth was defined as fetal death before onset of labor. Intrapartum death was defined as stillbirth when the fetus was alive at the start of labor. Early neonatal death refers to a death of a live-born infant within the first 7 days of life, while death covers the remaining period up to the first year of life. GA was determined as the best obstetric estimate based

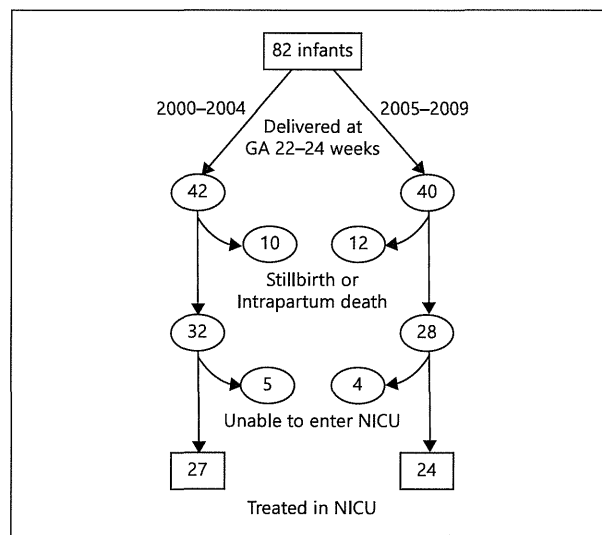


Fig. 1. Demographic characteristics of infants born at 22–24 weeks of GA delivered in 2000–2009 in our single institution. During the 10-year study period, 82 infants were delivered at GA 22–24 weeks, including 42 in 2000–2004 and 40 in 2005–2009. Of the 42 and 40 infants, 10 and 12 were stillbirths or intrapartum deaths, and the 32 and 28 were delivered as live-born infants. Of the 32 and 28 live-born infants, 5 and 4 were unable to enter the NICU because of severe asphyxia or extreme prematurity, and 27 and 24 were treated in the NICU.

on the last menstrual period, standard obstetric parameters, and ultrasonographic findings. Iatrogenic delivery represented a delivery medically or surgically induced due to maternal and/or fetal indications [8]. Antenatal steroid therapy was defined as the administration of any corticosteroid to the mother between GA 22 and 34 weeks for accelerating fetal lung maturation [9]. Surfactant administration included at least 1 dose of surfactant. Indomethacin treatment was conducted for closure of a patent ductus arteriosus (PDA) diagnosed critically or by echocardiography. Infants with body weight below the 10 percentile of the mean of the Japanese birth size standard data were classified as small for GA (SGA) [10].

Follow-up evaluations, including interval health history, neurologic evaluations, and developmental assessments (developmental quotient, DQ), were performed at 3 years of age. Developmental testing was performed using the Kyoto Scale of Psychological Development 2001 (KSPD) by trained testers. KSPD is a Japanese standard developmental test and is used to assess disabled children by most of public health centers [11]. It is an individualized face-to-face test administered by experienced psychologists to assess child's development in the following three areas: postural-motor (fine and gross motor functions); cognitive-adaptive (non-verbal reasoning or visuospatial perceptions assessed using materials such as blocks, miniature cars, and marbles), and language-social (interpersonal relationship, socializations and verbal abilities). DQ was calculated by dividing the developmental age by chronological

Table 1. Perinatal characteristics and interventions for 60 live-born infants at GA 22–24 weeks

	2000–2004 (n = 32)	2005–2009 (n = 28)	p value
<b>Obstetric characteristics</b>			
CAM or p-PROM	16 (50)	17 (61)	0.28
Preeclampsia	2 (6)	6 (21)	0.09
<b>Interventions</b>			
Iatrogenic preterm delivery	8 (25)	8 (29)	0.49
Tocolytic treatment	30 (94)	15 (54)	<0.01
Antenatal steroid	2 (6)	9 (32)	0.01
Cesarean section	12 (38)	15 (54)	0.16
<b>Neonatal interventions</b>			
Intubation at birth	25 (78)	24 (86)	0.34
Surfactant administration	19 (59)	20 (71)	0.24

Figures in parentheses indicate percentages. CAM = Chorioamnionitis; p-PROM = preterm premature rupture of membrane. Iatrogenic delivery means delivery was induced by maternal and/or fetal indications. Antenatal steroid therapy was defined as administration of any corticosteroid to the mothers between GA 22 and 34 weeks for accelerating fetal lung maturation.

age and then multiplying the quotient by 100. The mean and one standard deviation of DQ was 100.6 and 13.4, respectively. According to the protocol Japanese Society for Follow-up Study of High-Risk Infants, we defined as a normal or borderline developmental status a DQ score over 70, a mild status as a DQ from 50 to 70, and a moderate to severe status as a DQ less than 50 [12]. The study was approved by the Institutional Review Boards of Kyushu University.

#### Statistics

Differences between groups were tested for significance by the  $\chi^2$  test. Multivariate logistic regression analysis was conducted for survival over one year and normal to mild neurodevelopmental delay (DQ >50) as independent variables; dependent variables included perinatal characteristics, interventions and morbidities. Only dependent variables with a p value <0.25 on univariate analysis were entered into the multiple logistic models. The statistical analyses were conducted using Excel statistics (SSRI, Japan) for Windows and SPSS software (v19; SPSS, Chicago, Ill., USA). Results with p values <0.05 were considered significant.

#### Results

##### Survival of Infants Born at 22–24 Weeks of GA between 2000–2004 and 2005–2009

During the 10-year study period, a total of 82 infants were delivered at GA 22–24 weeks, including 42 in 2000–2004 and 40 in 2005–2009 (fig. 1). Ten and 12 of them

Table 2. Neonatal characteristics and interventions of survivors born at 22–24 weeks of GA over one year

	2000–2004 (n = 14)	2005–2009 (n = 19)	p value
<b>Neonatal characteristics</b>			
Male sex	8 (57)	9 (47)	0.84
Multiple birth	1 (7)	2 (11)	0.74
1-min Apgar score <4	8 (57)	16 (84)	0.18
5-min Apgar score <4	3 (21)	8 (42)	0.38
SGA	0 (0)	6 (32)	0.06
GA <24 weeks	6 (43)	7 (37)	0.50
Birthweight <400 g	0 (0)	2 (11)	0.32
<b>Interventions</b>			
High-frequency oscillation	10 (71)	19 (100)	0.05
Indomethacin	7 (50)	17 (89)	0.03
Ligation	3 (21)	6 (32)	0.80
Early parenteral nutrition	5 (36)	18 (95)	<0.01
Transfusion	13 (93)	19 (100)	0.88

Figures in parentheses indicate percentages. Infants with body weight below the 10 percentile of the mean of the Japanese birth size standard data were classified as SGA. Indomethacin treatment was performed for the closure of PDA diagnosed clinically or by echocardiography.

were stillbirths or intrapartum deaths, and 32 and 28 were delivered as live-born infants in 2000–2004 and 2005–2009, respectively. In 2000–2004, 18 (56%) infants died within 365 days of life including 15 early (0–6 days) and 3 late (7–27 days) neonatal deaths, and 14 (44%) survived over one year. In 2005–2009, 9 (32%) infants died, including 7 early and 1 late neonatal death, and 19 (68%) survived to 1 year. This difference in survival rate is statistically significant ( $p = 0.04$ ). When perinatal characteristics and interventions were compared, the 32 live-born infants in the second period underwent less frequently maternal tocolysis (54 vs. 94%,  $p < 0.01$ ) and more frequently antenatal steroid therapy (32 vs. 6%,  $p = 0.01$ ) than 28 born in the first period (table 1). No other profile differed significantly between the two groups (table 2).

##### Survival Factors for Infants Born at 22–24 Weeks of GA

When neonatal characteristics and interventions were compared between the 14 (in 2000–2004) and 19 (in 2005–2009) survivors, the post-2005 survivors received more frequently indomethacin therapy (89 vs. 50%,  $p = 0.03$ ) and early parenteral nutrition (95 vs. 36%,  $p < 0.01$ ) than the pre-2004 ones (table 2).

Table 3. Clinical variables associated with a DQ >50 at 3 years of age

Variable	Infants born at 22–24 weeks of GA treated in NICU (n = 48 <sup>1</sup> )					
	univariate			multivariate		
	OR	95% CI	p value	OR	95% CI	p value
GA <24 weeks	0.19	0.05–0.67	0.02	0.14	0.03–0.67	0.01
Parenteral nutrition	4.82	1.38–16.76	0.02	1.01	0.09–10.78	0.99
Ligation	7.88	1.42–43.66	0.03	0.19	0.01–2.39	0.20
Transfusion	9.47	1.10–81.73	0.05	8.87	0.97–81.37	0.05
High-frequency oscillation	5.19	1.00–26.95	0.08	5.24	0.45–61.75	0.19
Indomethacin	2.43	0.74–7.98	0.24	9.75	0.67–141.9	0.10
1-min Apgar score <4	0.45	0.12–1.63	0.37			
Male sex	0.59	0.18–1.90	0.56			
Birthweight <400 g	3.29	0.28–39.16	0.70			
Iatrogenic preterm delivery	1.21	0.34–4.29	0.77			
5-min Apgar score <4	0.68	0.19–2.43	0.78			
Multiple birth	0.56	0.10–3.26	0.82			
SGA	1.17	0.23–5.94	0.85			
Cesarean section	1.11	0.35–3.54	0.86			
Tocolytic treatment	0.89	0.24–3.37	0.86			
Antenatal steroid	1.37	0.35–5.34	0.92			

OR = Odds ratio; CI = confidence interval. Logistic regression analysis was used to investigate the independent variables on a DQ >50. Obstetric characteristics and interventions, neonatal characteristics and interventions with a p value <0.25 on univariate analysis were entered into the multivariate logistic models.

<sup>1</sup> Three patients in whom neurodevelopmental status was not evaluated were excluded.

### Neurological Morbidity of Survivors Born at 22–24 Weeks of GA at 3 Years of Age

Three patients (1 in the first and 2 in the second period) were not evaluated because of moving or being treated for malignancy. Seven (54%) of 13 evaluable survivors attained a normal or borderline developmental status (DQ >70) in 2000–2004, and 7 (41%) of 17 survivors obtained that level in 2005–2009. Four (31%) infants in the pre-2004 group and 7 (41%) in the post-2005 group had a moderate or severe developmental delay (DQ <50). The proportion of infants who attained a DQ >50 did not reach statistical significance in the first and the second study period (69 vs. 59%,  $p = 0.84$ ).

### Neurodevelopmental Factors for Attaining a DQ >50 at 3 Years of Age

The attainment of a DQ >50 in survivors at 3 years of age was negatively associated with GA <24 weeks ( $p = 0.02$ ), and positively associated with ductus ligation ( $p = 0.02$ ) and parenteral nutrition ( $p = 0.03$ ) when assessed by univariate analysis. Multivariate analysis indicated a significant association only with GA <24 weeks ( $p = 0.01$ ; table 3).

### Discussion

The survival rate of infants born at GA 22–24 weeks increased significantly from 52 to 79% in a tertiary center during the decade studied. In addition, the percentage of SGA increased from 0 to 32% between the two periods. The improved survival might be due to the prenatal management including the restraint of tocolytic treatment and the more extensive use of antenatal steroid therapy, as well as to the neonatal management such as the promotion of indomethacin treatment and parenteral nutrition. However, at 3 years of age survivors born in 2005–2009 did not attain a more favorable neurodevelopment than those born in 2000–2004. The premature birth at GA <24 weeks was the most critical factor influencing neurodevelopment in survivors.

Antenatal steroid therapy has been reported to decrease the mortality of infants with GA 22–25 weeks [7, 13]. Prophylactic indomethacin may have short-term benefits for preterm infants including a reduction in the incidence of symptomatic PDA, PDA surgical ligation, and severe IVH [14]. From 2006, we routinely introduced indomethacin prophylaxis for preterm infants born at

<25 weeks of GA to reduce the risk of intraventricular hemorrhage. However, the timing of administration varied with the clinical condition of patients or individual physician preference. The nutritional problems of preterm infants have become particularly relevant to survival from NICU, as numerous studies have underlined the importance of parenteral nutrition for short- and long-term neurodevelopmental outcomes. The post-2005 survivors received more high-frequency oscillation therapy (71 vs. 100%,  $p = 0.05$ ) than the pre-2004 ones. However, it is controversial to what extent indomethacin, parenteral nutrition and high-frequency oscillation could affect the mortality of these infants [15].

In the present study, although the survival of preterm infants at the limit of viability increased significantly over a decade, the neurodevelopment of the survivors (DQ >50), did not improve, and actually it deteriorated from 69 to 59%. However, since the total number of survivors who attained a borderline or normal development (DQ >70) was small, this trend did not reach statistical significance or was it possible to evaluate it with a multivariate analysis. We did not have enough infants in our single institute to evaluate survival and neurodevelopmental outcome at GA 22, 23 and 24 weeks. There are a few reports on the neurological outcome of survivors at GA 22 weeks [6, 16]. The cohort study of the Neonatal Research Network, Japan, revealed that the proportion of unimpaired or minimally impaired was 12.0% at GA 22 weeks and 20.0% at GA 23 weeks [17]. Infants born at GA 22–25 weeks are fragile and vulnerable to medical interventions because of the extreme immaturity of organ sys-

tems. If the survival rate increases and the neurodevelopmental impairment remains the same, the absolute number of infants with neurological problems will increase. However, the guideline for resuscitation of preterm infants at the limit of viability is still used in Japan. Based on the presented data, the probability of not only survival but also neurodevelopmental outcome of these infants is vital for counseling parents, informing care, and planning service. Recently, a prospective follow-up study of very low-birthweight infants in Japan has revealed that periventricular leukomalacia, gastrointestinal perforation, intraventricular hemorrhage, and moderate or severe bronchopulmonary dysplasia correlated with the developmental delay at 3 years of age [12]. Brain development occurs actively during the second and third trimesters of fetal life, with neurogenesis, neural migration, maturation, apoptosis, and synaptogenesis [18, 19]. Repeated courses of antenatal steroids have a promoting effect on the myelination in developing nonhuman primate brain [20]. Further studies are required to explore the significant association of antenatal steroids with long-term neurodevelopmental outcome in the light of their possible neuroprotective effects.

#### Acknowledgements

This study was supported in part by a grant from the Kyushu University Clinical Research Network Project, and the Japan Ministry of Education (No. 24791113). We thank Dr. Hideki Nakayama and Dr. Shunji Hikino for their involvement in the management of the preterm infants.

#### References

- Hakansson S, Faroqi A, Holmgren PA, Serenius F, Hogberg U: Proactive management promotes outcome in extremely preterm infants: a population-based comparison of two perinatal management strategies. *Pediatrics* 2004;114:58–64.
- Hintz SR, Kendrick DE, Vohr BR, Poole WK, Higgins RD, Neo NICHD: Changes in neurodevelopmental outcomes at 18 to 22 months' corrected age among infants of less than 25 weeks' gestational age born in 1993–1999. *Pediatrics* 2005;115:1645–1651.
- Hoekstra RE, Ferrara TB, Couser RJ, Payne NR, Connett JE: Survival and long-term neurodevelopmental outcome of extremely premature infants born at 23–26 weeks' gestational age at a tertiary center. *Pediatrics* 2004;113:e1–e6.
- Markestad T, Kaarensen PI, Ronnestad A, Reigstad H, Lossius K, Medbo S, Zanussi G, Englund IE, Sjaerven R, Irgens LM: Early death, morbidity, and need of treatment among extremely premature infants. *Pediatrics* 2005;115:1289–1298.
- Fellman V, Hellstrom Westas L, Norman M, Westgren M, Kallen K, Lagercrantz H, Marsal K, Serenius F, Wennergren M: One-year survival of extremely preterm infants after active perinatal care in Sweden. *JAMA* 2009;301:2225–2233.
- Itabashi K, Horiuchi T, Kusuda S, Kabe K, Itani Y, Nakamura T, Fujimura M, Matsuo M: Mortality rates for extremely low birth weight infants born in Japan in 2005. *Pediatrics* 2009;123:445–450.
- Mori R, Kusuda S, Fujimura M: Antenatal corticosteroids promote survival of extremely preterm infants born at 22 to 23 weeks of gestation. *J Pediatr* 2011;159:110–114.e111.
- Goldenberg RL, Culhane JF, Iams JD, Romero R: Epidemiology and causes of preterm birth. *Lancet* 2008;371:75–84.
- Roberts D, Dalziel S: Antenatal corticosteroids for accelerating fetal lung maturation for women at risk of preterm birth. *Cochrane Database Syst Rev* 2006;■■:CD004454.
- Yoshida SH, Unno N, Kagawa H, Shinozuka N, Kozuma S, Taketani Y: Sonographic determination of fetal size from 20 weeks of gestation onward correlates with birth weight. *J Obstet Gynaecol Res* 2001;27:205–211.
- Tamaru S, Kikuchi A, Takagi K, Wakamatsu M, Ono K, Horikoshi T, Kihara H, Nakamura T: Neurodevelopmental outcomes of very low birth weight and extremely low birth weight infants at 18 months of corrected age associated with prenatal risk factors. *Early Hum Dev* 2011;87:55–59.